Multi-Objective Optimal Operation Planning for Battery Energy Storage in a Grid-Connected Micro-Grid

Anto Ryu, Hideo Ishii, and Yasuhiro Hayashi
Department of Advanced Science and Engineering, Waseda University, Tokyo, Japan
Email: ryu-anto@akane.waseda.jp; hideishii@aoni.waseda.jp; hayashi@waseda.jp

Abstract—**This paper investigates an evaluation of the expected business continuity for a grid-connected micro-grid (GCMG) consisting of a photovoltaic (PV) system and a Battery Energy Storage System (BESS) during an interruption of the external power supply. For evaluation indices, duration of self-power supply for critical loads and success rate of uninterrupted self-power supply are adopted and investigated in relation to PV capacity and BESS initial charge. In addition, a novel method of multi-objective optimal operation planning for BESS in a GCMG is proposed in this paper. Operation cost and resilience, which exist in a trade-off relationship, are simultaneously considered within the micro-grid. Electricity purchasing cost from the grid is used as an index of operation cost, duration of power outage within the micro-grid while switched to an independent operation state is used as an index of resilience to formulate the multi-objective optimization problem to determine the BESS operation planning. For optimization method, Multi-Objective Particle Swarm Optimization (MOPSO) is adopted. To verify the effectiveness of the proposed method, the numerical simulation was conducted, and the results demonstrated that the Pareto solutions, obtained by the proposed method, proved useful to micro-grid operators to determine the BESS operation planning considering the best balance between operation cost and resilience, which meet their need.**

Index Terms—**Battery energy storage, micro-grid, Multi-Objective Particle Swarm Optimization (MOPSO), optimal operation planning, resilience**

I. Introduction

Natural disasters such as earthquakes and typhoons are prone to cause serious damage to electric power systems, in the worst scenario, interruptions of external power supply could occur. In recent years, Central America and the Southeastern United States have been victims of periodic large-scale hurricanes and have suffered damage to both electric power systems and society in general [1]. In other case, Japan is an earthquake-prone country, and the 2011 Great East Japan Earthquake [2] together with the effects of the accompanying tsunami, caused widespread power outages from the epicenter to the relatively distant Tokyo area. In 2018, a large-scale earthquake occurred in Hokkaido area in the vicinity of the main regional thermal power plants. Emergency stops of multiple generators resulted in a prefecture-wide blackout. Although the conditions varied, the blackout lasted for several days, even in places that experienced no physical damage. Therefore, to ensure a stable power supply for local infrastructures, it is critical to either avoid blackouts as far as possible, or to reduce the recovery time when blackouts occur. In other words, there is a need to improve power supply resilience.

Against this backdrop, there has been an increasing focus on micro-grids. A micro-grid is a small-scale power supply system integrating power generation and load management systems [3]. The effects of the external power supply interruption may be avoided by engaging a micro-grid to self-power supply in the event of a blackout, if the micro-grid's power generating systems remain intact. In general, micro grids are used as energy systems in non-electrified remote islands and developing countries where there is a lack of power infrastructure and power supply costs are high [4]. In our present advanced information society, there is a growing need for a Business Continuity Plan (BCP) in office buildings and industrial plants to ensure that basic business operations can continue even when the external power supply is interrupted by natural disasters. Thus, the concept of building micro-grids in specific areas, depending on the required level of power supply resilience for the facilities, is spreading. In Japan's earthquake-prone capital city of Tokyo, the Ordinance for Measures Concerning Stranded Persons [5] requires that employees be accommodated within the offices for 72 hours after a disaster for the sake of safety and the BCP during the interim. Thus, a facility's ability to provide its own energy, and the length of time it can operate in isolated conditions are critical indices for the resilience of micro-grids. This issue has previously been addressed by [6] through the installation of emergency generators along with a fixed stockpile of fuel, but environmental concerns make it more likely that micro grids combining photovoltaic (PV) systems and other increasingly cost-effective forms of renewable energy with battery energy storage system (BESS) will be pursued.

Manuscript received September 8, 2019; revised October 30, 2019; accepted November 20, 2019.
Corresponding author: Anto Ryu (email: ryu-anto@akane.waseda.jp).

doi: 10.18178/ijeetc.9.3.163-170

Therefore, a grid-connected micro-grid (GCMG) consisting of PV and BESS is dealt with in this paper. We investigate the GCMG that switches to an independent micro-grid (IMG) state from an interruption of the external power supply during emergencies and plays a role to provide by its own power. For constructing GCMG, there is a demand to determine the required size of PV and BESS capacity in order to minimize operation cost during normal periods and satisfy the required duration of self-power supply during emergency periods at the same time. The key to this approach is in the control of highly operable BESS.

Some previous studies have been performed on minimizing the BESS capacity within the micro-grid for specific purposes [7]-[9]. Some studies have been performed on optimal operation planning for GCMG to minimize operation cost accounting for time-of-use electricity rates [10]-[19] during normal periods, and optimal operation planning for IMG focusing on resilience and BCP [20]-[23] during emergency periods. However, few studies have dealt with the optimal operation planning for GCMG simultaneously considering both operation cost and resilience, although there were cases in which they have been evaluated in combination with operation cost and the total load which was not supplied after the external power supply has been interrupted [24].

In this paper, an evaluation of the expected business continuity for existing GCMG based on the actual facility operation is investigated. The duration that GCMG is able to self-power supply after switching to an IMG state and the success rate of uninterrupted self-power supply for critical loads are used as evaluation indices for the level of resilience. Further investigation is then conducted on how these two evaluation indices changed with changing PV capacity and BESS initial charge. Furthermore, numerical simulations are conducted to examine operation cost during normal periods when time-of-use electricity rates are applied, along with the duration of self-power supply during emergency periods, for a fixed size of PV and BESS capacity. These two indices exist in a trade-off relationship and cannot be simultaneously optimized. Therefore, the multi-objective optimization approach is used, and the Pareto solutions of multi-objective optimal operation planning for BESS are obtained. Based on the results, a novel method is proposed to determine the multi-objective optimal operation planning for BESS in a GCMG accounting for both operation cost and resilience.

The rest of this paper is organized as follows. In Section II, an evaluation of the expected business continuity for GCMG is described. In Section III, the multi-objective optimization problem accounting for operation cost and resilience to determine BESS operation planning is formulated. Finally, in Section IV, conclusions are drawn based on the results of conducted numerical simulations.

II. Evaluation of Expected Business Continuity for Grid-Connected Micro-Grid

In this section, the system model of GCMG dealt with in this paper was summarized. In addition, the evaluation method and results of expected business continuity for GCMG was described.

A. System Model of Grid-Connected Micro-Grid

The system model of GCMG dealt with in this paper was the research center belonging to the Obayashi Corporation hosting large-scale test facilities with 500 kW and 300 kW power consumptions, a 457-kW co-generation system, an 820 kW PV system, and a 500 kW/3000 kWh BESS [25]. The annual maximum power consumption is approximately 2500 kW. The PV power is either accumulated in the BESS or consumed internally on site. When the external power supply is interrupted, a circuit breaker at the grid connection point is opened, a switch is made to an IMG, and the power in the BESS along with that generated by the PV at that time is supplied to power the facility. The BESS within GCMG operates to minimize the operation cost under the basic contract rate with the power companies during normal operation. In addition, basic business operations may be continued for a fixed time during a blackout by using emergency power for general office work. During a blackout, power use is restricted as necessary: computer use is limited to essential work, external communication such as by telephone or internet remains available, utilities such as certain toilets and lights are retained, etc. The critical load on the IMG was assumed to be a constant 40 kW, based on assumptions such as the number of people performing work during emergencies as well as the actual test imitating the emergency. In addition, an assumption was made that gas supply would also be interrupted and that co-generation would not be available. Fig. 1 shows a schematic diagram of GCMG. In IMG state, electricity power is supplied to critical loads by the PV system, and excesses or deficiencies are handled by matching consumption and supply through control of BESS charging and discharging. When surplus PV power arose from a fully charged BESS or capacity constraints, PV output curtailment is engaged. When PV power generation was at a low level, and the energy stored in BESS was exhausted, the MG experiences a power outage until the external power supply recovers.

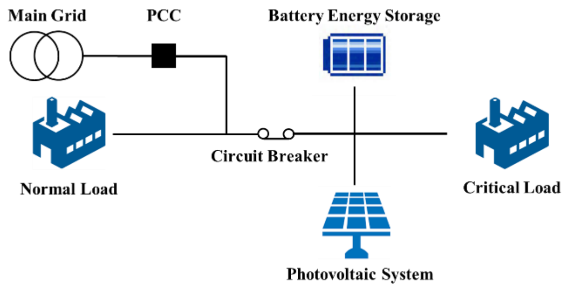

Fig. 1. Schematic diagram of grid-connected micro-grid.

B. Evaluation Method

The relationship between the duration of self-power supply and duration of power outage within the micro-grid, while the external power supply is interrupted, are formulated as

$$K = \mathrm{DSS}_t + \mathrm{DPO}_t \tag{1}$$

where K is the duration in hour from the interruption to the recovery of the external power supply. DSS_t is the duration in hour of self-power supply within the micro-grid when the external power supply is interrupted at time t. DPO_t is the duration in hour of power outage when the external power supply is interrupted at time t.

In this paper, the duration of self-power supply can be calculated by the flowchart in Fig. 2. In addition, Fig. 3 also illustrates the state change of the main grid and micro-grid over time.

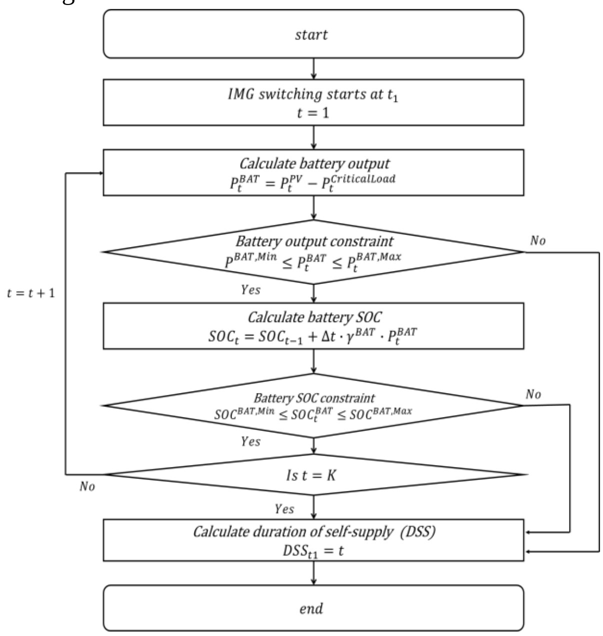

Fig. 2. Control process flowchart for PV and BESS during IMG switching.

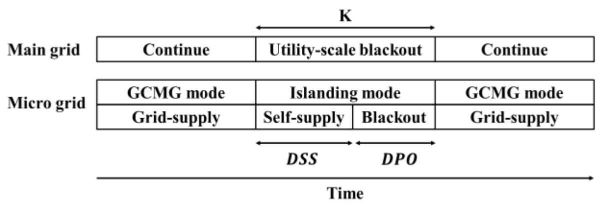

Fig. 3. State change of main grid and micro-grid over time.

Since it is difficult to predict the timing of the interruptions of the external power supply due to natural disasters such as earthquakes and typhoons, it is necessary to identify and evaluate the worst-case scenario in which duration of self-power supply is at its lowest. Here, the timing of the interruptions of the external power supply was set as PM6 in this paper, since the PV power generation recovery time is longest, and it leads duration of self-power supply to its lowest. From this time onward, the facility switches to the IMG and supplies power to critical loads, numerical simulations are conducted in which each day of the year becomes the starting point to evaluate how long the facility can self-power supply by itself to evaluate the expected business continuity for GCMG.

In the above settings, PV power generation was not expected until the following morning after switching to IMG, and it was assumed that the only power source was the BESS. Therefore, the SOC of BESS greatly affected the duration of self-power supply at the time of IMG switching. In terms of maximizing the minimum value of duration of self-power supply after IMG switching annually, while reliably minimizing operation cost during normal periods, the SOC of BESS at the time point of PM6 should be enlarged as much as possible during everyday BESS operation. This issue has been investigated in the authors' prior research [26]. Using real annual data, the authors performed BESS operations satisfying the capacity (500 kW/3000 kWh) and the maximum value of annual power supply from the grid (1500 kW or less), while avoiding surplus PV power generation, and maximizing the minimum SOC at PM6 annually. Based on the results, the minimum SOC of BESS at PM6 was 974 kWh during operation throughout the year.

For the first evaluation index, DSS^{Min} was defined as the minimum value of DSS_t. For the second evaluation index, RBC(n) was defined as the number n of days annually expressed as a percentage on which business continuity is possible after switching to IMG at PM6. Here, a 7-day period was assumed as K, the duration of the external power supply recovery from power outage, to evaluate the worst-case scenario of business continuity, although it is much longer than most of actual cases. An evaluation of how DSS^{Min} and RBC(7) changed depending on the PV capacity and BESS initial charge at IMG switching was then performed.

Here, the rated input and output of BESS was assumed to be 500 kW. The round-trip efficiency of BESS was assumed to be 70%. The PV capacity and BESS initial charge were set as shown in Table I. PV power generation was then determined from the annual data obtained from a real 820 kW system according to the capacity. The critical loads after IMG switching was assumed to be a constant 40 kW. This evaluation is general one with a constant load, which is free from the detail of the IMG but is just relevant to the PV capacity (kW) and BESS initial charge (kWh), then all the investigation and results are displayed for a 1 kW unit load used continuously. Correspondence with absolute values is obtained by multiplying by a factor of 40 which is a constant value of critical loads at this numerical simulation.

TABLE I: EXAMINED CAPACITY OF PV AND BESS

PV rated output (kW)	BESS initial charge (kWh)
0 - 3000 (250 increments, 13 ways)	0 - 3000 (250 increments, 13 ways)

C. Evaluation Results

Fig. 4 shows the relationship between PV capacity, BESS initial charge and DSS^{Min} per 1 kW unit load. In Fig. 4, a combination of system capacities is shown in which each point satisfies the desired shortest duration of self-power supply. For example, DSS^{Min}=72 hours (3 days) can be achieved if PV capacity is 31.25 kW and BESS initial charge is 56.25 kWh. Furthermore, Fig. 5 shows the relationship between PV capacity and DSS^{Min} when BESS initial charge is fixed at 24.35 kWh (rated capacity 75 kWh). From these results, it was found that per unit load, 1 kW PV capacity had approximately 0.1-

hour effect on DSS^{Min} on average. Fig. 6 shows the relationship between BESS initial charge and DSS^{Min} per unit load when the PV capacity was fixed at 75 kW. From this figure, per unit load, a 1 kWh BESS initial charge had about 1.32-hour effect on DSS^{Min} on average. It is proposed that the 1 kWh storage quantity's effect of one hour or more on the 1 kW load supply was due to an increase in the number of cases in which next-day PV power generation time was reached as a result of extended supply availability.

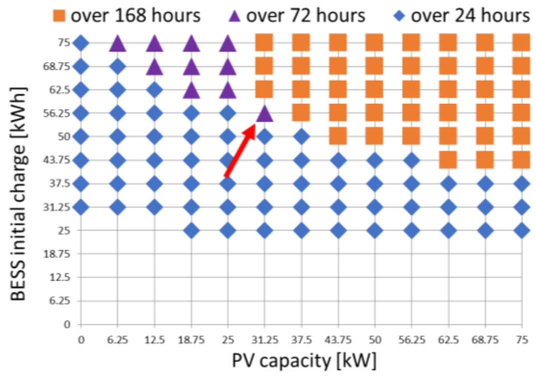

Fig. 4. Relationship between PV capacity/BESS initial charge and DSS^{Min} per unit load.

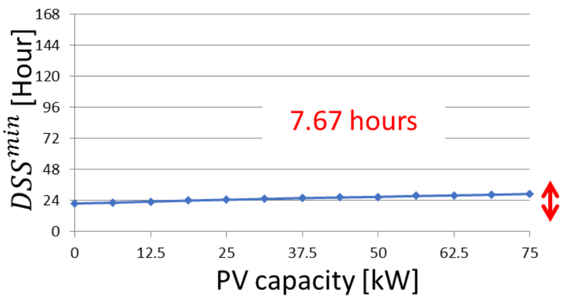

Fig. 5. Relationship between PV capacity and DSS^{Min} per unit load (BESS initial charge = 24.35 kWh).

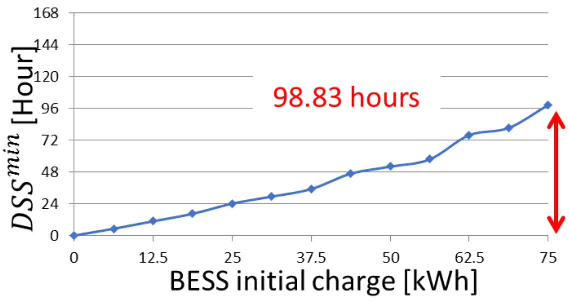

Fig. 6. Relationship between BESS initial charge and DSS^{Min} per unit load (PV capacity = 75 kW).

Similarly, Fig. 7 shows the relationship between PV capacity, BESS initial charge and RBC(7) per 1 kW unit load. In Fig. 7, a combination of system capacities is shown in which each point satisfies the desired success rate of uninterrupted self-power supply. For example, PV capacity=18.75 kW and BESS initial charge=25 kWh corresponds to a capacity combination satisfying RBC(7) =80%. Furthermore, Fig. 8 shows the relationship between PV capacity and RBC(7) assuming BESS initial charge=24.35 kWh (rated capacity is 75 kWh). As an example, from this figure, per unit load, PV needs to be 18.75 kW in order to realize RBC(7)>80%. In addition, we find that RBC(7) increases dramatically from 6.25 kW to 18.75 kW in PV capacity. It is believed that this is due to a dramatic increase in the number of cases in which abundant surplus PV power was generated during the daytime, making it possible to fully charge the BESS. From this result, it is seen that from 6.25 kW to 18.75 kW in PV capacity, the sensitivity to the 7-day success rate of uninterrupted self-power supply is high, as is the PV cost-benefit ratio from a BCP perspective. Fig. 9 shows the relationship between BESS initial charge and RBC(7) when the PV capacity is fixed at 75 kW. For example, from this result, it can be seen that BESS initial charge needs to be 31.25 kWh or higher per unit load to satisfy RBC(7)>80%. In addition, from the figure, RBC(7) is 0 until BESS initial charge is close to 12.5 kWh. This is so because if SOC of BESS is not 12.5 kWh or higher, the BESS consumes all the stored energy at some moment before the next morning. In addition, it was found that BESS initial charge of between 12.5 kWh and 25.75 kWh, the rise in RBC(7) is high, as is the cost-benefit ratio. It can be said that the investigated evaluation method was applicable to any setting based on the number of days of business continuity. It was found that there were high cost-to-benefit effects in certain instances for PV and BESS capacity in terms of resilience as described above.

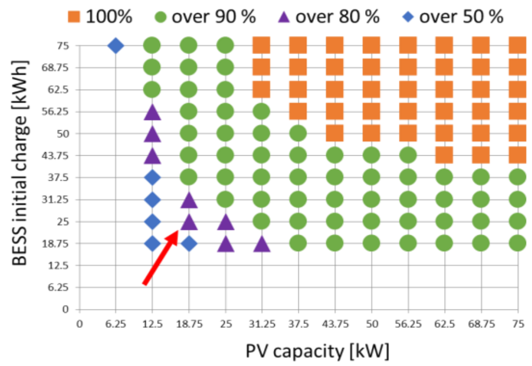

Fig. 7. Relationship between PV capacity/BESS initial charge and RBC(7) per unit load.

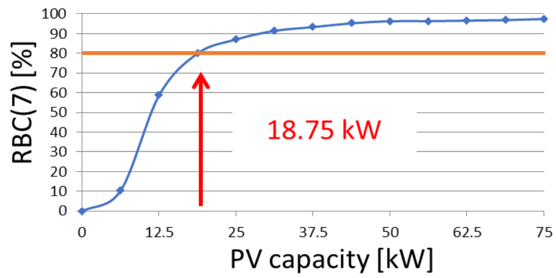

Fig. 8. Relationship between PV capacity and RBC(7) per unit load (BESS initial charge = 24.35 kWh).

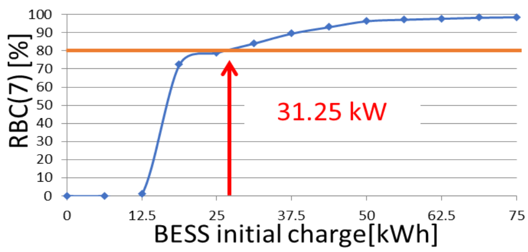

Fig. 9. Relationship between BESS initial charge and RBC(7) per unit load (PV capacity = 75 kW).

III. Multi-Objective Optimal Operation Planning for Battery Energy Storage

In this section, a novel method of the multi-objective optimal operation planning for BESS in a GCMG accounting for operation cost and resilience was proposed.

A. Problem Formulation

Operation cost during normal periods and resilience during emergency periods after IMG switching exist in a trade-off relationship. Moreover, these two indices cannot simply be measured on the same scale. Therefore, the multi-objective optimization approach was adopted in this paper. The multi-objective optimization problem dealt with in this paper was formulated as follows. An objective function was established for each index of operation cost and resilience. Electricity purchasing cost from the grid was used as an index of operation cost, duration of power outage within the micro-grid after IMG switching was used as an index of resilience to be minimized. These two objective functions were expressed by

$$\mathrm{OC} = \sum_{t=1}^{T} U_t \Delta t \left(P_t^{\text{Normal Load}} + P_t^{\text{Critical Load}} + P_t^{\text{BAT}} - P_t^{\text{PV}} \right) \quad (2)$$

$$\mathrm{DPO} = \frac{1}{T} \sum_{t=1}^{T} (K - \mathrm{DSS}_t) \quad (3)$$

The constraints were expressed by

$$P_t^{\text{BAT, Min}} \le P_t^{\text{BAT}} \le P_t^{\text{BAT, Max}} \quad (4)$$

$$\mathrm{SOC}_{t+1}^{\text{BAT}} = \mathrm{SOC}_t^{\text{BAT}} + \frac{\Delta t P_t^{\text{BAT}} \gamma^{\text{BAT}}}{E^{\text{BAT}}} \times 100 \quad (5)$$

$$\gamma^{\text{BAT}} = \begin{cases} \gamma^{\text{BAT}} & \text{if } P_t^{BAT} > 0 \\ \dfrac{1}{\gamma^{\text{BAT}}} & \text{if } P_t^{BAT} < 0 \end{cases} \quad (6)$$

$$\mathrm{SOC}_t^{\text{BAT,Min}} \le \mathrm{SOC}_t^{\text{BAT}} \le \mathrm{SOC}_t^{\text{BAT,Max}} \quad (7)$$

$$\mathrm{SOC}_1^{\text{BAT}} = \mathrm{SOC}_T^{\text{BAT}} \quad (8)$$

$$P_t^{\text{Normal Load}} + P_t^{\text{Critical Load}} + P_t^{\text{BAT}} - P_t^{\text{PV}} = 0 \quad (9)$$

where, OC is operation cost (JPY/day), U_t is electricity unit price at time t (JPY/kWh), t is time point from 1 to T, Δt is time steps (one-hour) (hour), $P_t^{\text{Normal Load}}$ is power of normal loads at time t (kW), $P_t^{\text{Critical Load}}$ is power of critical loads at time t (kW), P_t^{PV} is power of PV at time t (kW), P_t^{BAT} is charging and discharging power of BESS at time t (kW), DPO is duration of power outage (hour).

The optimization variables were set as the charging and discharging power of BESS at each time.

For the objective function DPO in (3), the mean value of the duration of power outage experienced at each time point (here, one-hour increments) was adopted to consider the uncertainty of the timing of the external power supply interruption.

Equation (4) shows the maximum and minimum limit constraints on BESS charging and discharging power at time t. Equation (5) shows the SOC of BESS at time t. Equation (6) shows the charging and discharging efficiency of BESS. Equation (7) shows the maximum and minimum limit constraints on the SOC of BESS at time t. Equation (8) shows the starting and ending value match constraints for the SOC of BESS, which reflects continuous daily facility operation. Equation (9) shows the supply and demand balance match constraint within the micro-grid.

The multi-objective optimization problem as described above was solved using a heuristic optimization method of Multi-Objective Particle Swarm Optimization (MOPSO) [27], and the Pareto solutions of multi-objective optimal operation planning for BESS considering operation cost and duration of power outage were obtained. However, when calculations were made with MOPSO, initial solutions were randomly determined based on random numbers. Among these initial solutions, optimal solutions were pre-included in which both operation cost and duration of power outage were each minimized though. An optimal solution for operation cost minimization was obtained by solving the linear programming problem formulated in (2) and (4) to (9), except (3), using a MATLAB linear optimization solver [28]. In other hand, an optimal solution for duration of power outage minimization was obtained based on the scheduled operation described in (8) and (10), such that the emergency power supply would last for as long as possible even when the external power supply was interrupted at any time; in other words, the BESS always charges at full level. In this way, the Pareto solutions of the multi-objective optimal operation planning for BESS can be obtained with ensuring an optimal solution for both indices.

$$P_t^{\text{BAT}} = E^{BAT} \frac{\mathrm{SOC}_{t+1}^{\text{BAT,Max}} - \mathrm{SOC}_t^{\text{BAT}}}{100} \cdot \frac{1}{\gamma^{\text{BAT}}} \quad (10)$$

B. Numerical Simulation Conditions

The numerical simulation was conducted to verify the effectiveness of the proposed method of the multi-objective optimal operation planning for BESS. The condition settings were as follows: PV and BESS capacity were set to 820 kW and 500 kW/500 kWh respectively. The time-of-use electricity rates for business sector used by the Tokyo Electric Power Company (TEPCO) in Japan [29] was adopted. High rates for daytime and low rates for nighttime were set as shown in Table II. Fig. 10 and Fig. 11 show the PV system and total load profiles. Two days were selected as typical days from one year of facility operation results with and without surplus PV power. The time increment was set as one-hour. Note that, selling electricity of PV surplus power to the grid was considered as free of charge.

TABLE II: TIME-OF-USE ELECTRICITY RATES

Time [Hour]	Unit price [JPY/ kWh]
0:00-8:00	12
8:00-22:00	18
22:00-24:00	12

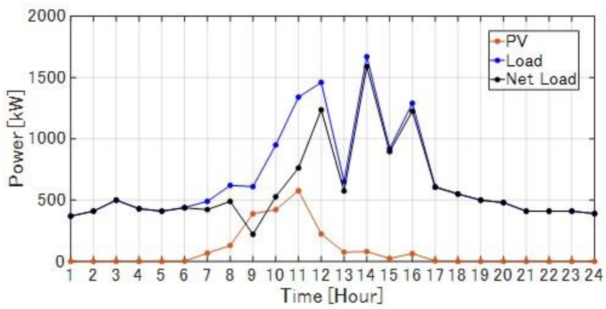

Fig. 10. Typical non-surplus PV power days.

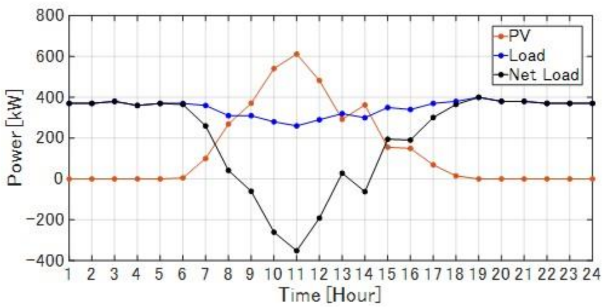

Fig. 11. Typical surplus PV power days.

C. Numerical Simulation Results

Fig. 12 shows the multi-objective optimal operation planning for BESS, obtained by the proposed method, on non-surplus PV power days. Yellow indicates operation cost minimization, green indicates duration of power outage minimization, and blue indicates a typical Pareto solution for both indices. The yellow operation planning for operation cost minimization assumes no surplus PV power, so there is a full charge from early in the morning, and complete discharge occurs sometime past noon when the electricity unit price is high. The green operation planning for duration of power outage minimization assumes that there are always preparations for emergencies of the external power supply interruption, and BESS maintained a fully charged state from early in the morning until night. The blue Pareto solution indicates an intermediate behavior in both operation cost and duration of power outage reduction. As the degrees of required resilience increases, time periods with high SOC of BESS increase and the timing of BESS discharge is delayed in time periods with higher unit price. Fig. 13 shows the cases on surplus PV power days. Since selling electricity of surplus PV power to the grid is considered as free of charge, and does not contribute to operation cost reduction, BESS discharged in the morning whatever the operation planning is adopted. This ensures spare charging capacity of BESS to charge the surplus PV power. Similar to non-surplus PV power days, as the degrees of required resilience increases, time periods with high SOC of BESS increase and the timing of BESS discharge is delayed in time periods with higher unit price.

Fig. 14 shows the Pareto solutions for the multi-objective optimal operation planning for BESS, obtained by the proposed method, on non-surplus PV power days, accounting for operation cost and duration of power outage. It can be confirmed that operation cost in normal periods and duration of power outage in emergency periods exist in a trade-off relationship for BESS operation planning. Similarly, the Pareto solutions on surplus PV power days were shown in Fig. 15. We propose the Pareto solutions to be a helpful tool for micro-grid operators to determine the multi-objective optimal operation planning for BESS considering the best balance between cost and resilience, which meet their need.

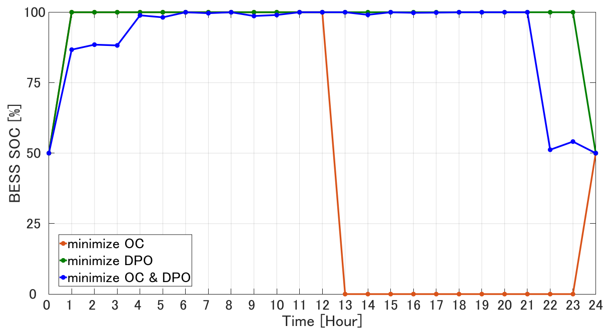

Fig. 12. Multi-objective optimal operation planning for battery energy storage on non-surplus PV power days.

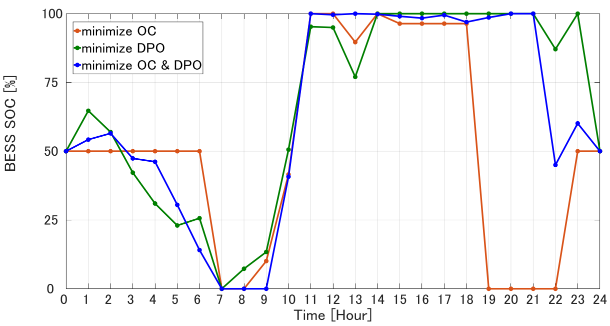

Fig. 13. Multi-objective optimal operation planning for battery energy storage on surplus PV power days.

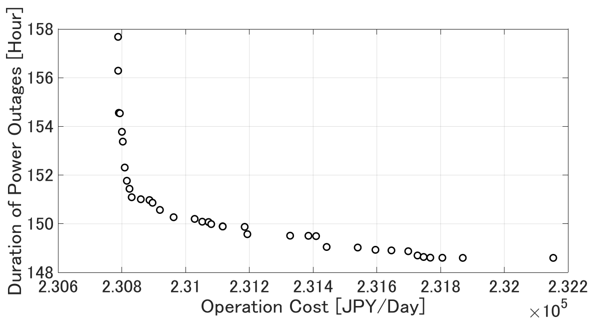

Fig. 14. Pareto solutions for multi-objective optimal operation planning for battery energy storage on non-surplus PV power days.

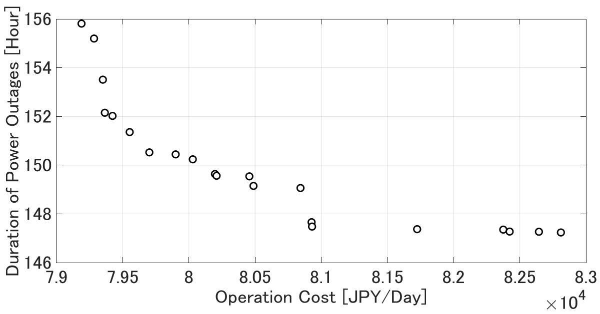

Fig. 15. Pareto solutions for multi-objective optimal operation planning for battery energy storage on surplus PV power days.

IV. Conclusions

In this paper, the evaluation of the expected business continuity for GCMG consisting of PV and BESS during the interruption of the external power supply was investigated. The relationship between PV capacity, BESS initial charge, and the duration of self-power supply after switching to IMG was evaluated and found that there were high cost-to-benefit effects in certain instances for PV and BESS capacity in terms of resilience. In addition to that, the multi-objective optimal operation planning for BESS in a GCMG was proposed. The numerical simulation results demonstrated that the Pareto solutions, obtained by the proposed method, proved useful to micro-grid operators to determine the multi-objective optimal operation planning for BESS considering the best balance between operation cost and resilience, which meet their need.

Conflict of Interest

The authors declare no conflict of interest.

Author Contributions

Anto Ryu conducted the research and wrote the paper. Hideo Ishii and Yasuhiro Hayashi gave advises and revised the paper. All authors had approved the final version.

Acknowledgment

The authors would like to acknowledge the financial support from Graduate Program for Power Energy Professionals, Waseda University from MEXT WISE Program, Japan. They also express their thanks to Mr. H. Onojima of Obayashi Corporation for supporting the research.

References

[1] E. S. Blake, T. B. Kimberlain, R. J. Berg, J. P. Cangialosi, and J. L. Beven II. "Tropical cyclone report hurricane sandy," National Hurricane Center. Feb. 2013.

[2] N. Nojima, "Restoration processes of utility lifelines in the Great East Japan Earthquake Disaster," presented at 15th World Conference on Earthquake Engineering, 2012.

[3] CERTS. CERTS Microgrid Concept. [Online]. Available: https://certs.lbl.gov/initiatives/certs-microgrid-concept

[4] Okinawa Electric Power Company. Distributed Energy Systems in Okinawa remote islands. [Online]. Available: http://www.env.go.jp/nature/biodic/ecdisso2014/pdf/subcommittee2/simabukuro.pdf

[5] Tokyo Metropolitan Government. Ordinance for Measures Concerning Stranded Persons. [Online]. Available: http://www.bousai.metro.tokyo.jp/kitaku_portal/1000672/1000731.html

[6] Ismail Kasikci, *Analysis and Design of Low-Voltage Power Systems: An Engineer's Field Guide*, WILEY-VCH, 2004.

[7] L. N. An, Q. T. Tran, B. Seddik, and V. L. Nguyen, "Optimal sizing of a grid-connected microgrid," in *Proc. IEEE International Conference on Industrial Technology*, 2015, pp. 2869-2874.

[8] T. A. Nguyen, M. L. Crow, and A. C. Elmore, "Optimal sizing of a vanadium redox battery system for microgrid systems," *IEEE Trans. on Sustainable Energy*, vol. 6, no. 3, pp. 729-737, 2015.

[9] H. Jahangir, A. Ahmadian, and M. A. Golkar, "Multi-objective sizing of grid-connected micro-grid using Pareto front solutions," in *Proc. IEEE Innovative Smart Grid Technologies Asia*, 2015, pp. 1-6.

[10] M. Sechilariu, F. Locment, L. Trigueiro, and D. Santos, "A conceptual framework for full optimal operation of a grid-connected DC microgrid," in *Proc. IEEE Int. Conf. on Industrial Electronics for Sustainable Energy Systems*, 2018, pp. 296-301.

[11] S. Aslam, N. Javaid, M. Asif, U. Iqbal, Z. Iqbal, and M. A. Sarwar, "A mixed integer linear programming based optimal home energy management scheme considering grid-connected microgrids," in *Proc. 14th International Wireless Communications & Mobile Computing Conference*, 2018, pp. 993-998.

[12] C. Liu, X. Wang, Y. Zou, H. Zhang, and W. Zhang, "A probabilistic chance-constrained day-ahead scheduling model for grid-connected microgrid," in *Proc. North American Power Symposium*, 2017, pp. 1-6.

[13] Z. Li and Y. Xu, "Dynamic dispatch of grid-connected multi-energy microgrids considering opportunity profit," in *Proc. IEEE Power & Energy Society General Meeting*, 2017, pp. 1-5.

[14] A. C. Luna, N. L. Diaz, M. Savaghebi, W. Feng, K. Sun, J. C. Vasquez, and J. M. Guerrero, "Generation and demand scheduling for a grid-connected hybrid microgrid considering price-based incentives," in *Proc. 43rd Annual Conference of the IEEE Industrial Electronics Society*, 2017, pp. 2498-2503.

[15] A. T. Eseye, D. Zheng, H. Li, and J. Zhang, "Grid-price dependent optimal energy storage management strategy for grid-connected industrial microgrids," in *Proc. Ninth Annual IEEE Green Technologies Conference*, 2017, pp. 124-131.

[16] L. N. An and Q. T. Tran, "Optimal energy management for grid connected microgrid by using dynamic programming method," in *Proc. IEEE Power & Energy Society General Meeting*, 2015, pp. 1-5.

[17] A. L. N. Diaz, M. Savaghebi, J. C. Vasquez, J. M, Guerrero, K. Sun, G. Chen, and L. Sun, "Optimal power scheduling for a grid-connected hybrid PV-wind-battery microgrid system," in *Proc. IEEE Applied Power Electronics Conference and Exposition*, 2016, pp. 1227-1234.

[18] S. Sirouspour, "Optimal scheduling of a storage device in a grid-connected microgrid using stochastic chance-constraint optimization," in *Proc. 42nd Annual Conference of the IEEE Industrial Electronics Society*, 2016, pp. 2100-2105.

[19] L. Bai, Q. Hu, F. Li, T. Ding, and H. Sun, "Robust mean-variance optimization model for grid-connected microgrids," in *Proc. IEEE Power & Energy Society General Meeting*, 2015, pp. 1-5.

[20] D. E. Olivares, C. A. Canizares, and M. Kazerani, "A centralized energy management system for isolated microgrids," *IEEE Trans. on Smart Grid*, vol. 5, no. 4, pp. 1864-1875, 2014.

[21] V. Sarfi and H. Livani, "A novel multi-objective security-constrained power management for isolated microgrids in all-electric ships," in *Proc. IEEE Electric Ship Technologies Symposium*, 2017, pp. 148-155.

[22] L. T. D. Santos, M. Sechilariu, and F. Locment, "Day-ahead microgrid optimal self-scheduling: Comparison between three methods applied to isolated DC microgrid," in *Proc. 40th Annual Conference of the IEEE Industrial Electronics Society*, 2014, pp. 2010-2016.

[23] H. Farzin, M. Fotuhi-Firuzabad, and M. Moeini-Aghtaie, "Developing a stochastic approach for optimal scheduling of isolated microgrids," in *Proc. 23rd Iranian Conference on Electrical Engineering*, 2015, pp. 1671-1676.

[24] H. Farzin, M. Fotuhi-Firuzabad, and M. Moeini-Aghtaie, "A stochastic multi-objective framework for optimal scheduling of energy storage systems in microgrids," *IEEE Trans. on Smart Grid*, vol. 8, no. 1, pp. 117-127, 2017.

[25] Obayashi Corporation Technical Research Institute. Facilities Introduction. [Online]. Available: https://www.obayashi.co.jp/tri/

[26] H. Maruyama, H. Ishii, Y. Hayashi, H. Onojima, and Y. Kojima, "Study on business continuity capability by cooperative operation of photovoltaic and battery energy storage system," in *Proc. IEEE*

PES Asia-Pacific Power and Energy Engineering Conference, 2015, pp. 1-5.

[27] C. A. C. Coello and M. S. Lechuga, "MOPSO: A proposal for multiple objective particle swarm optimization," in *Proc. Congress on Evolutionary Computation*, 2002, vol. 2, pp. 1051-1056.

[28] MathWorks. MATLAB Optimization Solver. [Online]. Available: https://jp.mathworks.com/help/optim/ug/linprog.html

[29] Tokyo Electric Power Company. Time of Use Menu. [Online]. Available: http://www.tepco.jp/ep/private/plan2/old03.html

Anto Ryu received the B.E. degree in electrical engineering from Waseda University, Tokyo, Japan, in 2017. He is currently pursuing the Ph.D. degree in electrical engineering. His research interests include smart grid, micro grid operation, and battery control. He is a student member of the Institute of Electrical Engineers in Japan (IEEJ).

Hideo Ishii received the Ph.D. degree from the University of Tokyo, Tokyo, Japan, in 1996. He joined the Tokyo Electric Power Company (TEPCO), Tokyo, Japan, in 1988. He was a Visiting Scientist at the Massachusetts Institute of Technology, Cambridge, MA, USA from 1989 to 1991. From 2010, he has been engaged in some major smart-grid-related national projects in Japan as an organizer. He is now a Professor with the Advanced Collaborative Research Organization for Smart Society (ACROSS) at Waseda University, Tokyo, Japan. His current activities are in the field of electric energy systems, especially related to demand response and the integration of renewable energy resources. Prof. Ishii has been the Chief Director of the Japan ADR Association since 2013.

Yasuhiro Hayashi received the B.Eng., M.Eng., and D.Eng. degrees from Waseda University, Tokyo, Japan, in 1989, 1991, and 1994, respectively. In 1994, he became a Research Associate at Ibaraki University, Mito, Japan. In 2000, he became an Associate Professor at the Department of Electrical and Electronics Engineering, Fukui University, Fukui, Japan. He has been with Waseda University as a Professor of the Department of Electrical Engineering and Bioscience since 2009; and as a Director of the Research Institute of Advanced Network Technology since 2010. Since 2014, he has been a Dean of the Advanced Collaborative Research Organization for Smart Society at Waseda University. His current research interests include the optimization of distribution system operation and forecasting, operation, planning, and control concerned with renewable energy sources and demand response. Prof. Hayashi is a member of the Institute of Electrical Engineers of Japan and a regular member of CIGRE SC C6 (Distribution Systems and Dispersed Generation).